A novel soft hydrothermal (SHY) route to crystalline PbS and CdS nanoparticles exhibiting diverse morphologies†

Deborah Berhanu,[a] Kuveshni Govender,[a] David Smyth-Boyle,[a] Martin Archbold,[b] Douglas P. Halliday[b] and Paul O'Brien*[a]

Received (in Cambridge, UK) 6th September 2006, Accepted 11th October 2006
First published as an Advance Article on the web 25th October 2006
DOI: 10.1039/b612934j

We report a simple and rapid aqueous route to crystalline nanoparticles of PbS and CdS using single-source precursors and a conventional household pressure cooker.

There is considerable interest in developing simple, inexpensive and environmentally benign protocols (with control over issues such as phase purity, crystallinity and size distribution of products) to grow metal chalcogenide nanomaterials for practical use in *e.g.* light emitting diodes, non-linear optics, lasers and solar cells.[1] Semiconductor nanoparticles and quantum dots (QD's) of CdS and PbS are particularly well investigated.[2,3] Telecommunication and biological applications requires QD's that luminesce primarily in the NIR in the range 1300–1550 nm and 700–900 nm, consequently QD's based on semiconductors of Group IV–VI materials such as lead chalcogenides are particularly appealing. Factors include their small bulk bandgap (PbS 0.41 eV), ease of size tenability covering the NIR region and, in contrast to most II–VI and II–V semiconductors, lead chalcogenide QD's exhibit strong quantum size effects due to the large Bohr radii of both electrons and holes, leading to large confinement energies. Consequently, non-linear optical (NLO) behaviour within the confinement regime is expected to be significantly greater than for II–VI materials, thus attracting attention for optical switching and photonic devices. More recently, multiple exciton generation for PbS and PbS QD's has been reported, with potential to lead to an entirely new paradigm in high efficiency and low cost solar cell technology.[4]

Although both size *and* morphology determine the properties (and ultimately the potential applications) of semiconductor nanoparticles, the ability to direct or tailor the latter during nanoparticle growth processes remains comparatively underdeveloped in comparison to the former.[5] Addressing this issue would greatly facilitate further fundamental and interdisciplinary studies (*e.g.* comparison of the optoelectronic properties of nanorods, tubes, prisms, and cubes of similar dimensions for a single compound). In addition to the obvious benefits to nanotechnologists, new insights into crystal growth at the nanodimensional level would be expected.

[a]*School of Chemistry, University of Manchester, Manchester, UK M13 9PL. E-mail: paul.obrien@manchester.ac.uk; Fax: + 44 161 275 4616; Tel: +44 161 275 4652*
[b]*Department of Physics, University of Durham, Durham, UK DH1 3LE. E-mail: d.p.halliday@durham.ac.uk; Fax: +44 191 334 3585; Tel: +44 191 334 3571*

† Electronic supplementary information (ESI) available: Tables of experimental conditions, XRD and FT-IR. See DOI: 10.1039/b612934j

A variety of synthetic routes to semiconductors nanocrystals have been employed including solvothermal, arrested precipitation (*via* injection of organometallic precursors in hot coordinating solvents), chemical bath and sol–gel methods,[6] leading to different nanoparticle morphologies for CdS (*e.g.* nanorods, tetrapods, nanoprisms, *etc.*)[7] and PbS (nanocubes, nanorods, spherical, dendritic *etc.*).[8] Protocols that employ single-source (SS) precursors are attractive (*i.e.* air-stable, non-toxic and easy to handle) as they incorporate all the elementary constituents required to synthesise the final product in a single reagent and often employ clean, low-temperature decomposition routes to yield crystalline nanomaterials with minimal impurity incorporation.[9] A non-aqueous solution route to PbS nanoparticles involving amine-catalysed decomposition of SS precursors under ambient conditions has been reported recently.[10] Ostensibly environmentally-friendly approaches using aqueous solvents to deposit metal chalcogenide nanomaterials, such as "soft-chemical" solvothermal, or chemical bath methods often employ toxic chalcogenide precursors (*e.g.* thioacetamide, a potent hepatotoxin and carcinogen or sodium sulfide, which is harmful to aquatic species). In addition, the crystallinity of solution deposited materials is often poor, resulting in inferior optical and electronic characteristics.

We have previously grown CdS and PbS nanoparticles *via* the arrested precipitation–"hot-injection" method using metal bis-(dialkyldithiocarbamato) single source compounds in hot coordinating solvents.[11] In this Communication, we demonstrate a rapid, simple "soft-hydrothermal" (hereafter termed SHY) route to nanocrystalline PbS and CdS, using air stable crystalline complexes as SS precursors. The precursors chosen in this work (**A**: [2,2′-bipyridyl(Pb(SC(O)(C_6H_5)$_2$)]; **B**: [Pb(S_2(P(C_6H_5)$_2$)$_2$N)]); **C**: [2,2′-bipyridyl(Cd(SC(O)(C_6H_5)$_2$)]) readily decompose in aqueous media at low temperatures, which facilitates rapid nanoparticle synthesis using a conventional household steam pressure cooker. The as-demonstrated SHY procedure (*e.g.* non-reflux, air ambient, *etc.*) differs strongly from solvothermal approaches, which typically entail heterogeneous chemical reactions in the presence of a solvent at supercritical or near-supercritical conditions (and where varying solvents are required to lower temperature–pressure conditions).

Transmission electron micrographs of as-grown PbS nanocrystals are shown in Fig. 1. In the reactant concentrations and stoichiometries employed herein (‡ESI Table A†), it appears that morphological evolution of smooth faceted polyhedral nanocrystallites of PbS operates largely under kinetic control at low levels of supersaturation, thus avoiding emergence of dendritic morphologies (faceted polyhedral PbS nanoparticles with narrow

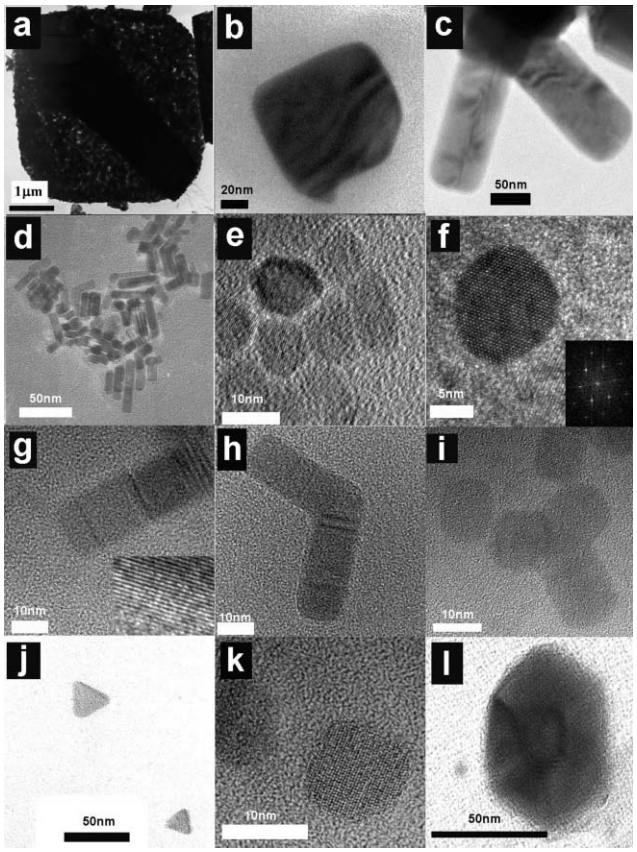

Fig. 1 TEM images obtained for PbS nanocrystals grown using precursors **A** (a–g) and **B** (h–l) using the soft-hydrothermal (SHY) route. Reaction conditions are given in ESI Table A.† For precursor **A**, increasing the thioglycerol : precursor ratio leads to formation of *a.* truncated cubes, *b.* rods and *c.* cubes , *d.* rods and *e.* hexagonal crystallites. Under less basic conditions and lower reactant concentrations, smaller *f.* hexagonal and *g.* rod crystals are formed. Similar results obtained using precursor **B**: *h.* bipods, *i.* tripods, *j.* prisms, *k.* tetradecahedrons and *l.* hexagonal bipyramids.

size distributions, rather than irregular fractal or "snowflake" morphologies, are desirable for efficient third-order NLO behaviour). Rapid decomposition of the precursor limits continuous nucleation.

In a typical experiment, an aqueous suspension containing the precursor metal complex, 1-thioglycerol and NaOH was prepared. Decomposition of the precursor was achieved using a conventional pressure-cooker. A variety of nanocrystalline materials could be prepared under different conditions (ESI Table A†). Using precursor **A**, cubic microcrystals (Fig. 1a) composed of smaller cubic nanocrystals (~40–45 nm) are formed. Moreover, precursor **A** can also be decomposed without additional base (NaOH), leading to smaller hexagonal (~12–15 nm, Fig. 1*f*) and rod-shaped (~10–40 nm in size, Fig. 1*g*) nanocrystals. Using a different precursor **B** and similar conditions, nanocrystals of PbS were also grown, including nanorods, bipods (Fig. 1*h*) and tripods (Fig. 1*i*), prisms (Fig. 1*j*), tetradecahedrons (Fig. 1*k*) and hexagonal bipyramids (Fig. 1*l*). Square and hexagonal facets could be indexed to {100} planes and trigonal facets to {111} planes through selected area electron diffraction (SAED). Data from powder X-ray diffraction (p-XRD) confirmed the crystalline nature of all materials obtained under the conditions described herein (ESI Fig. A†).

PbS crystallizes with the rocksalt structure (space group *Fm*3*m*, $a = 5.935$ Å).[3] The velocity of crystal growth for PbS is consistent with Bravais–Friedel–Donnay–Harker (BFDH) predictions and reported to follow the order {110} > {100} > {111};[8] the faster the growth in a given direction, the smaller the area of the face developed perpendicular to that direction. Solution grown PbS formed under conditions of low temperature and supersaturation, in the absence of growth modifiers, tends to develop *via* an initial cubic morphology, bounded by {100} planes, through several truncated forms and ultimately into octahedra bounded by slow growing {111} faces. Initial results obtained in the present work appear to show, however, that a variety of isotropic and anisotropic crystallites can be obtained through small variations in reagent concentrations and solution pH at fixed temperature and ambient pressure.

Several key trends can be identified, as exemplified using precursor **A**. As shown in ESI Table A,† at high pH, increasing the thioglycerol/precursor ratio (*i.e.* [TG] : [prec]) from ~74 : 1 to ~250 : 1 leads to the formation of different morphologies, in the order truncated cubes (Fig. 1a), rods and cubes (Fig. 1b and 1c) , rods (Fig. 1d) and hexagons (Fig. 1e). Lower pH and reagent concentrations tend to lead to smaller crystallites (see Fig. 1f and g). The solution pH influence is twofold; firstly, precursor decomposition is presumed to occur *via* nucleophilic attack of base on the electrophilic carbonyl carbon with concomitant weakening of the C–S bond and secondly, thioglycerol sorption on growing crystal faces (see below) is sensitive to solution pH.

The variety of crystallite morphologies obtained in the present study suggests thioglycerol acts as a growth modifying agent. When growth is inhibited in a direction perpendicular to a given face, the area of this face is expected to increase relative to the areas of other faces of the same crystal. Capping by thioglycerol, as evidenced by FT-IR data (ESI Fig. B†) would also be expected to impart a degree of both chemical stability and water solubility to PbS nanocrystals.[12] The overall pattern of results also suggests that low precursor concentrations, rather than large [TG] : [prec] values, may be more important for formation of nanorods. Moreover, as shown in Fig. 1g, nanorod morphologies can be observed at low pH ~ 5 (*i.e.* where thiol capping is expected to be less efficient) under conditions where shape anisotropy would not be expected to be promoted (thiols tend to sorb and impede growth of {111} faces rather than faster growing {100} faces of PbS).[13]

The optical and electronic characteristics of SHY-PbS nanoparticles were probed using low temperature photoluminescence (PL) spectroscopy. Work is ongoing and will be reported in detail elsewhere; briefly, non-radiative recombination was effectively suppressed and emission intensities were consistent with surface-passivated nanocrystals, furthermore spectral features were found to be sensitive to both particle morphology *and* dimensions. A representative PL spectrum of truncated hexagonal PbS nanocrystal samples (see Fig. 1a) prepared using precursor **A** is given in Fig. 2, showing strong emission bands centred at ~600, 700 and 880 nm, which are presumably band-edge related.[14] The high-energy end of the ~600 nm band (obtained using the 514 nm line of an Ar ion laser; 570 nm filter) is abridged; preliminary studies using higher excitation energy

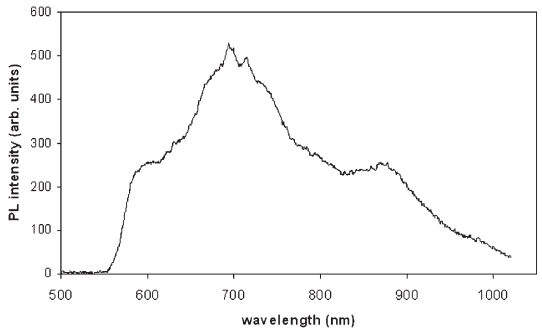

Fig. 2 Low temperature (4 K) PL spectrum of SHY-PbS nanocrystals grown using precursor **A** in the absence of additional base as shown in Fig. 1a. Reactant conditions given in ESI Table A.†

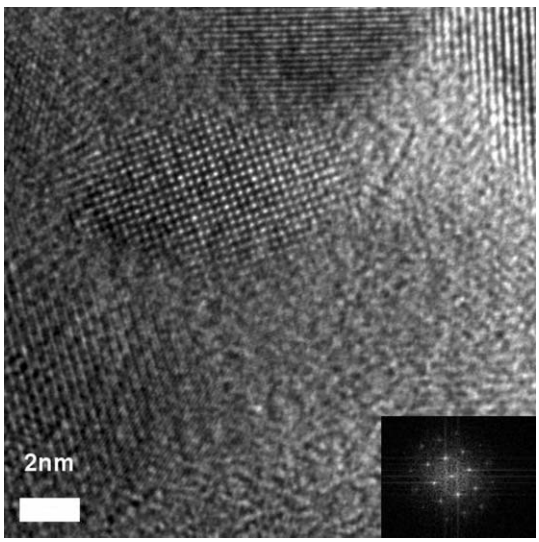

Fig. 3 TEM data for SHY-CdS nanocrystals. Inset shows SAED consistent with cubic CdS (JCPDS 75-0581) along the [001] zone axis.

(Ar 458 nm line) indicate PL bands extend to higher energy below ~600 nm.

The SHY approach has been extended to other metal chalcogenide nanoparticles, including CdS. In common with many Group II–IV semiconductors, CdS crystallizes with either the wurtzite structure [space group $C6_3mc$ (or C^4_{6v})] and hexagonal lattice (the thermodynamically stable phase) or the zincblende structure (hawleyite) with a cubic lattice, or polytypes thereof (*i.e.* similar cohensive energies). Hence unlike cubic PbS, CdS has an inherent tendancy to exhibit structural anisotropy, as reflected in the present work using precursor **C** ([2,2′-bipyridyl-(Cd(SC(O)(C_6H_5)$_2$)]). Water soluble CdS QD's have been prepared previously using **C** in deaerated basic solutions under reflux conditions.[12] In the present work, using experimental conditions similar to those employed for SHY-PbS (ESI Table 2†), elliptical nanocrystals were formed. Micrographs of oblate CdS nanocrystals (~7–12 nm) grown over periods of 10 min are shown in Fig. 3.

The simplicity of the outlined SHY approach provides potential for development of advanced materials with limited resources, using a single-step "one-pot" protocol with reduced energy consumption and air-stable precursors, thus appealing to chemists and others in the nanomaterials field and enabling further interdisciplinary studies. For example, as quantum confined PbS possesses simpler electronic properties compared to widely studied II–VI QD's, readily accessible synthetic protocols will facilitate experimental testing of different theoretical models of quantum confined nanostructures. Furthermore, the modest temperature and pressure conditions are compatible with syntheses of bioinspired materials.

Notes and references

‡ A Mettler Toledo MA 235 pH/ion analyser and InLab 413 electrode were used to record solution pH. X-Ray diffraction studies were performed using a Bruker AXS D8 diffractometer. Measurements were taken using 2θ values of 5–90° and a step size 0.01–0.02°. Scanning electron microscopy of carbon-coated samples was carried out on a Philips Excel 30 FEG SEM instrument. TEM electron microscopy was accomplished using a FEI Tecnai F30 FEGTEM (300 kV) or Philips CM200 (200 kV) microscope with an EDAX 9100 EDS unit. Electronic absorption spectra were obtained with a Helios Beta Thermospectronic spectrophotometer. Photoluminescence (PL) measurements were made at 4 K in a closed cycle helium cryostat using the 514 nm line of an argon ion laser and 570 nm filter.

Experimental: In a typical experiment, several Pyrex glass vials (10 cm^3) were charged with an aliquot of reaction solution containing the precursor metal complex, 1-thioglycerol and NaOH. Vessels were stoppered with a perforated polypropylene lid and placed within a support rack above the water level in a conventional pressure cooker (pre-heated to 100 °C). The apparatus was sealed and operating conditions (~2 atm, 121 °C) rapidly established. After the desired period (5–30 min), pressure was released and the reaction vessels removed. The resulting brown-black (PbS) or clear (CdS) solutions were poured immediately into an excess of cold (~5 °C) propan-2-ol to effect precipitation, the products separated by centrifugation and washed with water and propan-2-ol (washing with different solvents *e.g.* acetone, toluene, ethanol or hexane, results in the formation of large precipitates) before drying at ambient temperature and subsequent characterisation.

1 *The Chemistry of Nanomaterials*, ed. C. N. R. Rao, A. Müller and A. K. Cheetham, Wiley-VCH, Weinheim, 2004.
2 H. Weller, *Angew. Chem., Int. Ed. Engl.*, 1993, **32**, 41.
3 A. Lobo, T. Möller, M. Nagel, H. Borchert, S. G. Hickey and H. Weller, *J. Phys. Chem. B*, 2005, **109**, 17422.
4 G. R. J. Ellingson, M. C. Beard, J. C. Johnson, P. Yu, O. I. Micic, A. J. Nozik, A. Shabaev and A. L. Efros, *Nano Lett.*, 2005, **5**, 865.
5 C. Burda, X. Chen, R. Narayanan and M. A. El-Sayed, *Chem. Rev.*, 2005, **105**, 1025.
6 B. L. Cushing, V. L. Kolesnichenko and C. J. O'Connor, *Chem. Rev.*, 2004, **104**, 3893.
7 H. Chu, X. Li, G. Chen, W. Zhou, Y. Zhang, Z. Jin, J. Xu and Y. Li, *Cryst. Growth Des.*, 2005, **5**, 1801.
8 G. Zhou, M. Lü, Z. Xiu, S. Wang, H. Zhang, Y. Zhou and S. Wang, *J. Phys. Chem. B*, 2006, **110**, 6543.
9 N. L. Pickett and P. O'Brien, *Chem. Rec.*, 2001, **1**, 467.
10 Z. Zhang, S. H. Lee, J. J. Vittal and W. S. Chin, *J. Phys. Chem. B*, 2006, **110**, 6649.
11 T. Trindade, P. O'Brien, X. M. Zhang and M. Motevalli, *J. Mater. Chem.*, 1997, **7**, 1011.
12 Z. H. Zhang, W. S. Chin and J. J. Vittal, *J. Phys. Chem. B*, 2004, **108**, 18569.
13 S. M. Lee, Y. Jun, S. N. Cho and J. Cheon, *J. Am. Chem. Soc.*, 2002, **124**, 11244; S. M. Lee, S. N. Cho and J. Cheon, *Adv. Mater.*, 2003, **15**, 441.
14 J. H. Warner, A. R. Watt, M. J. Fernee, N. R. Heckenberg and H. Rubinsztein-Dunlop, *Nanotechnology*, 2005, **16**, 479 and references therein.